Dynamics of the pendulum with periodically varying length

Anton O. Belyakov, Alexander P. Seyranian, Angelo Luongo

Dynamics of the pendulum with periodically varying length

Anton O. Belyakov [a,*], Alexander P. Seyranian [a], Angelo Luongo [b]

[a] Institute of Mechanics, Moscow State Lomonosov University, Michurinsky pr. 1, Moscow 119192, Russia
[b] DISAT, Universita di L'Aquila, P. le Pontieri, Monteluco Roio 1, L'Aquila 67040, Italy

A B S T R A C T

Dynamic behavior of a weightless rod with a point mass sliding along the rod axis according to periodic law is studied. This is the pendulum with periodically varying length which is also treated as a simple model of a child's swing. Asymptotic expressions for boundaries of instability domains near resonance frequencies are derived. Domains for oscillation, rotation, and oscillation–rotation motions in parameter space are found analytically and compared with a numerical study. Chaotic motions of the pendulum depending on problem parameters are investigated numerically.

1. Introduction

Oscillations of a pendulum with variable length is among the classical problems of mechanics. Usually, the pendulum with periodically varying length is associated with a child's swing. As probably everyone can remember, to swing a swing one must crouch when passing through the middle vertical position and straighten up at the extreme positions, i.e. perform oscillations with a frequency which is approximately twice the natural frequency of the swing. Despite popularity of the swing, in the literature on oscillations and stability, where this problem is referred to in [1–5], there are not many analytical and numerical results on behavior of the pendulum with periodically varying length dependent on parameters. In [1] an approximate relation between the amplitude of a periodic orbit of the pendulum and the excitation frequency was found. In [2,3] the pendulum of variable length was cited as an example of a periodic system described by an equation different from the Mathieu equation but without further analysis. Change of energy and first instability region for the pendulum with variable piecewise constant length were discussed in [4]. An attempt to find the first instability region for the pendulum of variable length was undertaken in [5] but it is not correct. The stability analysis of the lower vertical position of the pendulum with damping and arbitrary periodic excitation function was carried out in [6]. In that paper the instability (parametric resonance) regions were found in the form of semi-cones in three-dimensional parameter space.

In papers [7,8] qualitative analysis of periodic solutions and their stability for a pendulum with periodically varying length, no damping, and arbitrary excitation amplitude was conducted. In these two papers the authors also discussed the adequacy of the pendulum with periodically varying length as a model of a swing.

The pendulum with periodically varying length is much less studied than the pendulum with oscillating support which is often referred to simply as a parametrically driven pendulum or parametric pendulum; see e.g. papers [9–11] and the references therein. These two pendula are described by different analytical models and consequently, possess different dynamical properties. For example, the pendulum with periodically varying length cannot be stabilized in the inverted vertical position; see Section 9. Nevertheless, the methods used for dynamical analysis of one pendulum are applicable for the other one. The methodological peculiarity of this work is in the assumption of quasi-linearity of the system for analytical study of its regular regimes which allows us to derive higher order approximations by the averaging method.

The present paper is devoted to the study of regular and chaotic motions of the pendulum with periodically varying length. Motivation of this work is investigating nonlinear dynamics of this rather simple but little studied pendulum and seeing what new dynamical effects are related to this model.

* Corresponding author. Tel.: +7 4959392039; fax: +7 4959390165.
E-mail addresses: a_belyakov@inbox.ru, anton.o.belyakov@gmail.com (A.O. Belyakov), seyran@imec.msu.ru (A.P. Seyranian), luongo@ing.univaq.it (A. Luongo).

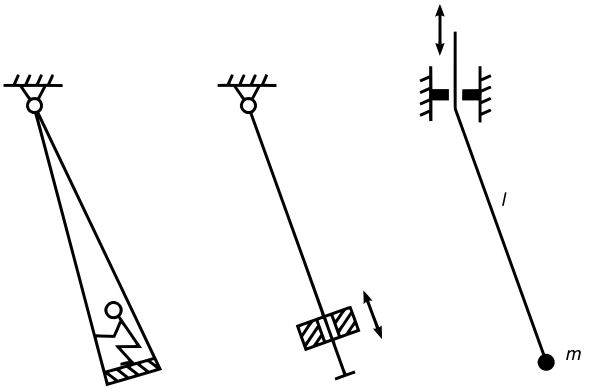

Fig. 1. Schemes of the pendulum with periodically varying length.

The paper is organized as follows. Main relations for the pendulum with periodically varying length are given in Section 2. Stability conditions of lower vertical position of the pendulum are found using the Floquet theory in Section 3. In Section 4 limit cycle solutions are obtained using the first approximation of Krylov–Bogolyubov averaging method for the quasi-linear oscillatory system. The stability conditions of limit cycles are derived in Section 5 based on Lyapunov's theorem of stability of periodic solutions. The adequacy of the pendulum with periodically varying length as a model of swing is discussed in Section 6. Existence conditions for regular rotations are found in Section 7 using the fifth approximation of averaging method, and these conditions are justified by numerical simulations. Regular rotation and rotation–oscillation regimes with various periods and mean angular velocities are recognized and discussed. In Section 8 domains for chaotic motions are found and analyzed in the parameter space numerically via calculation of Lyapunov exponents and Poincare maps. Major differences in the dynamics from the pendulum with fixed length and oscillating support are briefly discussed in Section 9.

2. Main relations

Equation for motion of the swing can be derived with the use of angular momentum alteration theorem; see [1–4]. Taking into account linear damping forces also, we obtain

$$\frac{\mathrm{d}}{\mathrm{d}t}\left(ml^2\frac{\mathrm{d}\theta}{\mathrm{d}t}\right)+\gamma l^2\frac{\mathrm{d}\theta}{\mathrm{d}t}+mgl\sin\theta=0, \tag{1}$$

where m is the mass, l is the length, θ is the angle of the pendulum deviation from the vertical position, g is the acceleration due to gravity, and t is the time (Fig. 1).

It is assumed that the length of the pendulum changes according to the periodic law

$$l=l_0+a\varphi(\Omega t),\qquad \int_0^{2\pi}\varphi(\tau)\mathrm{d}\tau=0, \tag{2}$$

where l_0 is the mean pendulum length, a and Ω are the amplitude and frequency of the excitation, $\varphi(\tau)$ is the smooth 2π-periodic function with zero mean value.

We introduce the following dimensionless parameters and variables

$$\tau=\Omega t,\qquad \varepsilon=\frac{a}{l_0},\qquad \Omega_0=\sqrt{\frac{g}{l_0}},\qquad \omega=\frac{\Omega_0}{\Omega},$$
$$\beta=\frac{\gamma}{m\Omega_0}. \tag{3}$$

Then, Eq. (1) can be written in the following form

$$\ddot\theta+\left(\frac{2\varepsilon\dot\varphi(\tau)}{1+\varepsilon\varphi(\tau)}+\beta\omega\right)\dot\theta+\frac{\omega^2\sin\theta}{1+\varepsilon\varphi(\tau)}=0. \tag{4}$$

Here the dot denotes differentiation with respect to new time τ. Behavior of the system governed by Eq. (4) will be studied in the following sections via analytical and numerical techniques depending on three dimensionless problem parameters: the excitation amplitude ε, the damping coefficient β, and the frequency ω under the assumption $\varepsilon\ll1,\beta\ll1$.

It is convenient to change the variable by the substitution

$$q=\theta(1+\varepsilon\varphi(\tau)). \tag{5}$$

Using this substitution in Eq. (4) and multiplying it by $1+\varepsilon\varphi(\tau)$ we obtain the equation for q as

$$\ddot q+\beta\omega\dot q-\frac{\varepsilon\left(\ddot\varphi(\tau)+\beta\omega\dot\varphi(\tau)\right)}{1+\varepsilon\varphi(\tau)}q+\omega^2\sin\left(\frac{q}{1+\varepsilon\varphi(\tau)}\right)=0. \tag{6}$$

This equation is useful for stability study of the vertical position of the pendulum as well as analysis of small oscillations.

3. Instability of the vertical position

Let us analyze the stability of the trivial solution $q=0$ of the nonlinear equation (6). Its stability with respect to the variable q is equivalent to that of Eq. (4) with respect to θ due to relation (5). According to Lyapunov's theorem on stability based on a linear approximation for a system with periodic coefficients the stability (instability) of the solution $q=0$ of Eq. (6) is determined by the stability (instability) of the linearized equation

$$\ddot q+\beta\omega\dot q+\frac{\omega^2-\varepsilon\left(\ddot\varphi(\tau)+\beta\omega\dot\varphi(\tau)\right)}{1+\varepsilon\varphi(\tau)}q=0. \tag{7}$$

This equation explicitly depends on three parameters: ε, β and ω. Expanding the ratio in (7) into Taylor's series and keeping only first order terms with respect to ε and β we obtain

$$\ddot q+\beta\omega\dot q+\left[\omega^2-\varepsilon(\ddot\varphi(\tau)+\omega^2\varphi(\tau))\right]q=0. \tag{8}$$

This is Hill's equation with damping with the periodic function $-(\ddot\varphi(\tau)+\omega^2\varphi(\tau))$. It is known that instability (i.e. parametric resonance) occurs near the frequencies $\omega=k/2$, where $k=1,2,\ldots$. Instability domains in the vicinity of these frequencies were obtained in [12,13] analytically. In three-dimensional space of the parameters ε, β and ω, these domains are described by half-cones

$$(\beta/2)^2+(2\omega/k-1)^2<r_k^2\varepsilon^2,\quad \beta\ge0,k=1,2,\ldots, \tag{9}$$

where $r_k=\frac{3}{4}\sqrt{a_k^2+b_k^2}$ is expressed through the Fourier coefficients of the periodic function $\varphi(\tau)$

$$a_k=\frac{1}{\pi}\int_0^{2\pi}\varphi(\tau)\cos(k\tau)\mathrm{d}\tau,$$
$$b_k=\frac{1}{\pi}\int_0^{2\pi}\varphi(\tau)\sin(k\tau)\mathrm{d}\tau. \tag{10}$$

Inequalities (9) give us the first approximation of the instability domains of the vertical position of the swing. These inequalities were obtained in [6] using different variables.

Remark. For a general system of linear differential equations with periodic coefficients only first order terms in the series of a monodromy matrix with respect to small parameters contribute to the first non-degenerate approximation of instability domains; see [13]. That is why to obtain the first order approximation for the instability domains we can omit higher order terms in Eq. (7) and use Eq. (8).

Note that each kth resonance domain in relations (9) depends only on the kth Fourier coefficients of the periodic excitation

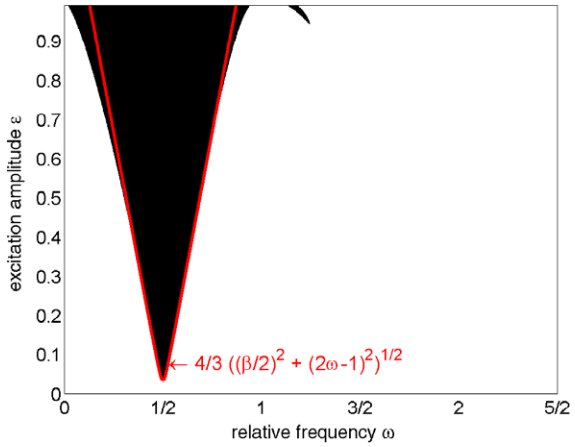

Fig. 2. Instability region of the pendulum with periodically varying length (red line) in comparison with numerical results (black area) on parameter plane (ω, ε) at $\beta = 0.05$.

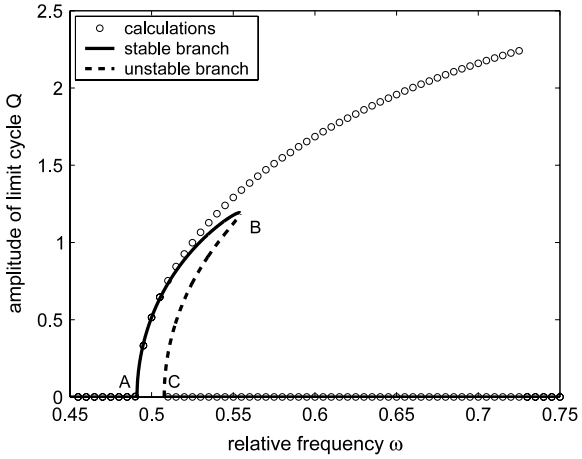

Fig. 3. Frequency-response curve for the parameters $\varepsilon = 0.04$ and $\beta = 0.05$. Amplitude Q of the limit cycle depending on the relative excitation frequency ω.

function. Particularly, for $\varphi(\tau) = \cos(\tau)$, $k = 1$ we obtain $a_1 = 1$, $b_1 = 0$, and $r_1 = 3/4$. Thus, the first instability domain takes the form

$$\beta^2/4 + (2\omega - 1)^2 < 9\varepsilon^2/16, \quad \beta \geq 0. \tag{11}$$

The boundary of the first instability domain ($k = 1$) is presented in Fig. 2 by the solid red line demonstrating a good agreement with the numerically obtained instability domain which is marked black. These boundaries are also drawn in Figs. 5, 6 and 8 by solid white lines. It is easy to see from (8) that for the second resonance domain ($k = 2$, $\omega = 1$) the excitation function $-(\ddot{\varphi}(\tau) + \omega^2\varphi(\tau))$ is zero for $\varphi(\tau) = \cos(\tau)$. This explains why the second resonance domain is empty, and the numerical results confirm this conclusion; see Fig. 2.

Inside the instability domains (9) the vertical position $q = 0$ becomes unstable and motion of the system can be either regular (limit cycle, regular rotation) or chaotic.

4. Motion at small excitation amplitude: Limit cycle

When the excitation amplitude ε is small, we can expect that the oscillation amplitude q in Eq. (6) is also small. We suppose that ε and β are small parameters of the same order as well as the factor of nonlinearity. Then, we can expand the sine into Taylor's series around zero in Eq. (6) and keep only two terms. Eq. (6) in the first approximation with respect to small parameters takes the following form

$$\ddot{q} + \beta\omega\dot{q} + \left[\omega^2 - \varepsilon(\ddot{\varphi}(\tau) + \omega^2\varphi(\tau))\right] q - \frac{\omega^2}{6} q^3 = 0. \tag{12}$$

Let us estimate the amplitude of the swing at which Eq. (12) is valid. Absolute value of the nonlinear term $\omega^2 q^3/6$ in Eq. (12) must be much less than the absolute value of the linear term $\omega^2 q$. Due to this condition we require that $q^2/6 < \varepsilon$. So, if we take $\varepsilon = 0.04$ then $|q| < \sqrt{0.24} \approx \pi/6$.

A limit cycle is a regular motion which can be studied with the assumption of small amplitudes of the system motion. We study the parametric excitation of nonlinear system (12) with the periodic function $\varphi(\tau) = \cos\tau$ at the first resonance frequency $\omega \approx 1/2$. We are looking for an approximate solution of system (12) in the form $q(\tau) = Q(\tau)\cos(\tau/2 + \Psi(\tau))$ using the averaging method for the resonance case [2] where $Q(\tau)$ and $\Psi(\tau)$ are the slow amplitude and phase. As a result, we get the system of averaged first order differential equations for the slow variables

$$\dot{Q} = -\frac{Q\beta\omega}{2} + \frac{Q\varepsilon(1-\omega^2)}{2}\sin(2\Psi), \tag{13}$$

$$\dot{\Psi} = \omega - \frac{1}{2} - \frac{Q^2\omega^2}{8} + \frac{\varepsilon(1-\omega^2)}{2}\cos(2\Psi). \tag{14}$$

This system gives steady solutions for $\dot{Q} = 0$, $\dot{\Psi} = 0$. Besides the trivial one $Q = 0$ we obtain expressions for the amplitude and phase as

$$Q^2 = \frac{4}{\omega^2}\left(2\omega - 1 \mp \sqrt{\varepsilon^2(1-\omega^2)^2 - \beta^2\omega^2}\right), \tag{15}$$

$$\Psi = \frac{1}{2}\arctan\left(\frac{\mp 4\beta\omega}{\sqrt{\varepsilon^2(1-\omega^2)^2 - \beta^2\omega^2}}\right) + \pi j, \tag{16}$$

where $j = \ldots, -1, 0, 1, 2, \ldots$ and "arctan" gives the major function value lying between zero and π.

To find boundaries of the resonance domain one should put $Q = 0$ in expression (15). These boundaries in the first approximation coincide with the boundaries of inequality (11). This is not a surprise because inequality (11) determines the first approximation of the instability domain for the trivial solution $Q = 0$. In Fig. 3 the amplitude–frequency response curve (15) is presented for the parameters $\varepsilon = 0.04$ and $\beta = 0.05$ in comparison with the numerical results (circles). Fig. 3 shows good agreement with the numerical simulations up to the amplitude equal to 1, which even exceeds the estimate $Q < \pi/6$ obtained above.

5. Stability of limit cycles

In order to study the stability of a periodic solution $q_0(\tau)$ we substitute it in Eq. (12) with small perturbation $q(\tau) = q_0(\tau) + \delta(\tau)$, and in the first approximation we obtain a linear differential equation for $\delta(\tau)$

$$\ddot{\delta} + \beta\omega\dot{\delta} + \left[\omega^2 + \varepsilon(1-\omega^2)\cos(\tau) - \frac{\omega^2}{2}q_0^2(\tau)\right]\delta = 0. \tag{17}$$

According to Lyapunov's theorem about stability based on the linear approximation the stability of the periodic solution $q_0(\tau)$ is governed by stability and instability of solutions $\delta(\tau)$ of linearized equation (17). This is Hill's equation with damping.

According to the averaging method [2] the periodic solution is presented as

$$q_0(\tau) = Q\cos(\tau/2 + \Psi) + \varepsilon u(\varepsilon, \tau, Q, \Psi), \tag{18}$$

where it is required that

$$\int_0^{4\pi} u(\varepsilon,\tau,Q,\Psi)\sin\left(\frac{\tau}{2}\right)\mathrm{d}\tau = \int_0^{4\pi} u(\varepsilon,\tau,Q,\Psi)\cos\left(\frac{\tau}{2}\right)\mathrm{d}\tau = 0 \tag{19}$$

in order to eliminate secular terms. We substitute (18) into (17), where Q and Ψ are taken from expressions (15) and (16). Then we get Hill's equation with damping (17) depending on three parameters $\omega \approx 1/2$, $\beta \ll 1$, and $\varepsilon \ll 1$ with 2π-periodic excitation function

$$\Phi(\tau) = (1-\omega^2)\cos(\tau) - \frac{Q^2\omega^2}{2\varepsilon}(\cos(\tau/2+\Psi))^2 + O(Q). \tag{20}$$

The term $O(Q) = O(\sqrt{\varepsilon})$ in principle contains all harmonics $1/2, 1, 3/2, \ldots$ and has a nonzero mean value. The first approximation of the instability domain for Eq. (17) in the vicinity of the point $\omega = 1/2, \beta = \varepsilon = 0$ has the form [12]

$$\beta^2/4 + (2\omega - 1 + a_0\varepsilon)^2 < \varepsilon^2(a_1^2 + b_1^2), \tag{21}$$

where the first Fourier coefficients of the function $\Phi(\tau)$ are the following

$$a_0 = -\frac{Q^2\omega^2}{2\varepsilon}, \tag{22}$$

$$a_1 = 1 - \omega^2 - \frac{Q^2\omega^2}{4\varepsilon}\cos(2\Psi), \tag{23}$$

$$b_1 = \frac{Q^2\omega^2}{4\varepsilon}\sin(2\Psi). \tag{24}$$

Here we have omitted higher order terms. Since $\omega \approx 1/2$ we can substitute the first term in inequality (21) by $\omega^2\beta^2$ and in the second term instead of $2\omega - 1$ insert $2\omega^2 - 1/2$. Near the values $\varepsilon = \beta = 0, \omega = 1/2$ a revised inequality remains valid

$$\omega^2\beta^2 + (2\omega^2 - 1/2 + a_0\varepsilon)^2 < \varepsilon^2(a_1^2 + b_1^2). \tag{25}$$

Substituting here the coefficients (22)–(24) and using expression for $\cos(2\Psi)$ from Eq. (14) with $\dot{\Psi} = 0$ we obtain the instability condition as

$$\mp Q^2\omega^2\sqrt{\varepsilon^2(1-\omega^2)^2 - \beta^2\omega^2} < 0 \tag{26}$$

which tells us that periodic solution (15) and (16) with the sign plus is stable and that with minus is unstable. These solutions are shown in Fig. 3 by solid and dashed lines, respectively. Circles in this figure indicate stable periodic and stationary solutions obtained by numerical integration with the use of the Runge–Kutta method. We note that unstable periodic solutions cannot be found by numerical integration of the initial value problem which is natural. We emphasize a good agreement between analytical and numerical results up to amplitudes $q \approx \pi/4$.

The presented proof of stability and instability of periodic solutions with the amplitude and phase given by Eqs. (15) and (16) is based on Lyapunov's theorem of stability of periodic solutions. Thus, this proof is *strict* and *direct* while in the literature on stability and vibrations usually the averaged (autonomous) equations are used with the stability analysis of fixed points; see e.g. [14]. Note that the stability study for the averaged equations (13) and (14) would give immediately condition (26).

In Fig. 3 at point A a supercritical Andronov–Hopf bifurcation occurs where the vertical position becomes unstable and a stable limit cycle appears. At point C a subcritical Andronov–Hopf bifurcation occurs where the vertical position becomes stable again and unstable periodic oscillatory solution appears. At point B meeting of stable and unstable solutions cause a saddle–node bifurcation where the limit cycle loses its stability.

6. On a model of swing

In the paper [7] periodic solutions of a pendulum with periodically varying length and no damping ($\beta = 0$) were considered, and the authors of [7] came to the conclusion that this pendulum cannot serve as a model of swing from the stability standpoint. However, in a recent paper the authors of [8] agree that a pendulum with periodically varying length independently on current angle of the pendulum can serve as a model of swing with this conclusion based on the qualitative analysis.

Let us discuss this question in detail. For the sake of simplicity we consider the case of resonance frequency $\Omega = 2\Omega_0$ ($\omega = 1/2$) for which according to (15) and (16) we have

$$Q^2 = 4\sqrt{9\varepsilon^2 - 4\beta^2}, \tag{27}$$

$$\Psi = \frac{1}{2}\arctan\left(\frac{2\beta}{\sqrt{9\varepsilon^2 - 4\beta^2}}\right) + \pi j, \quad j = 1, 2, \ldots \tag{28}$$

For small ratio β/ε we obtain

$$Q^2 = 12\varepsilon\left(1 - \frac{2\beta^2}{9\varepsilon^2}\right), \qquad \Psi = \frac{\beta}{3\varepsilon} + \pi j, \quad j = 1, 2, \ldots \tag{29}$$

This means that for the case of no damping ($\beta = 0$) the phase is equal to πj. Thus, at $\Omega = 2\Omega_0$ and $\beta = 0$ there exists the stable periodic motion $\theta(t) = Q\cos(\Omega_0 t)$ for which maximal deflection angle corresponds to maximal length of the swing, and minimal length corresponds to the vertical position of the swing. Perhaps, this motion looks unusual but according to (29) there is no other periodic solution. According to relation (29) inclusion of small damping leads to small positive phase shift and decreasing of the amplitude.

The periodic change of the length $l = l_0 + a\cos(2\Omega_0 t)$ is not optimal for fast pumping of the swing which is natural to expect. However, due to instability of the vertical position for the case of rather small damping, any child squatting and raising according to the periodic law $l = l_0 + a\cos(2\Omega_0 t)$ will pump the swing independently of the initial phase although with a small amplitude of the periodic motion. Thus, a pendulum with periodically varying length can be naturally treated as a model of swing. The presented arguments remain valid also for the frequencies Ω close to the resonance frequency $2\Omega_0$ and the periodic excitation function close to $\cos(2\Omega_0 t)$.

7. Regular rotations

We will say that the system performs regular rotations if a nonzero average rotational velocity exists:

$$b = \lim_{T\to\infty}\frac{1}{T}\int_0^T \dot{\theta}\,\mathrm{d}\tau.$$

Velocity b is a rational number because regular motions can be observed only in resonance with excitation. Motion with fractional average velocity such as $|b| = 1/2$ in Fig. 4(a) is usually called *oscillation–rotation*. Let us first study monotone rotations, where velocity $\dot{\theta}$ has constant sign and integer average value b; see Fig. 4(b) and (c). In order to describe resonance rotations of the pendulum with periodically varying length we will use the general averaging method [2,15] which requires rewriting (4) in the standard form as a system of first order equations with small right hand sides. For that reason we assume that ε, β and ω are small parameters, ε being of order ω^2, and β of order ω^3, which makes the system quasi-linear.

We introduce a vector of *slow* variables $\mathbf{x}$ and the fast time $s = b\tau$, where $x_1 = \theta - s$ is the *phase mismatch*, $x_2 = \dot{\theta}$ is the velocity, $x_3 = 1 + \varepsilon\cos(s/b)$ is the excitation, and dot denotes

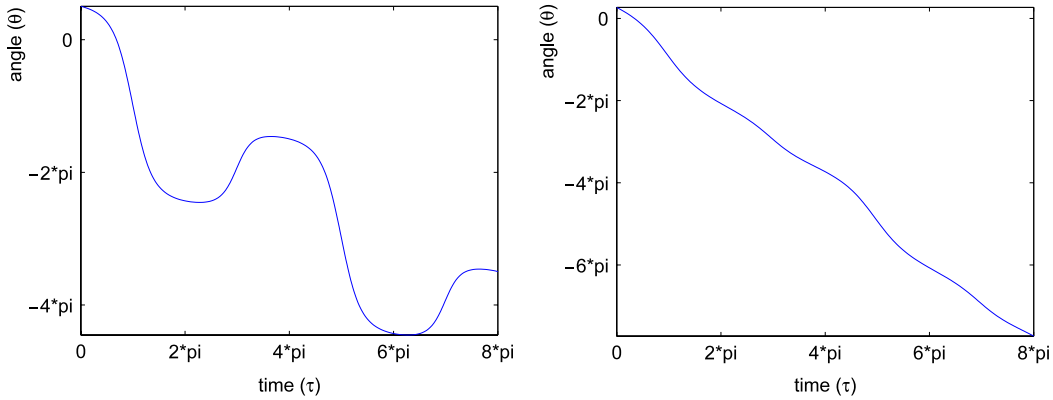

(a) $\varepsilon = 0.51, \omega = 0.54, \beta = 0.05$. (b) $\varepsilon = 0.28, \omega = 0.5, \beta = 0.05$.

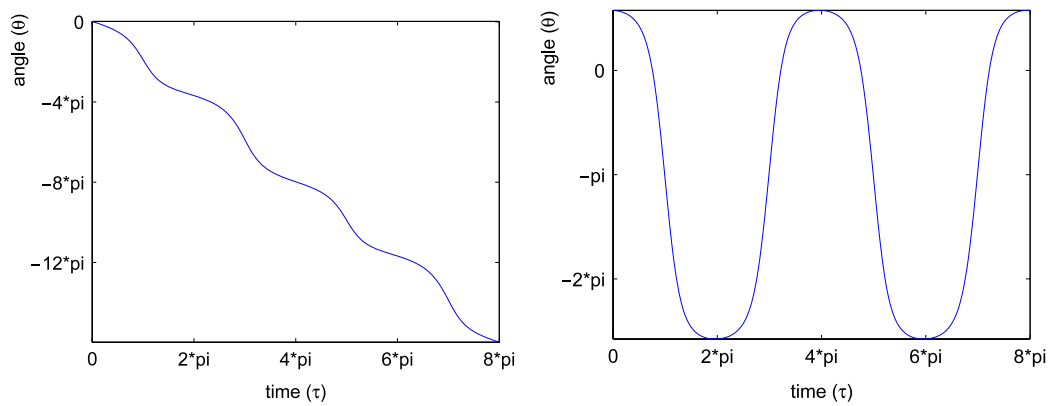

(c) $\varepsilon = 0.43, \omega = 0.5, \beta = 0.05$. (d) $\varepsilon = 0.59, \omega = 0.6, \beta = 0.05$.

Fig. 4. (a) Regular rotation–oscillation with the mean angular velocity equal to one half of the excitation frequency, $b = -1/2$. (b) Regular rotation with $b = -1$. (c) Regular rotation with $b = -2$. (d) Regular rotation–oscillation with $b = 0$.

derivative with respect to the new time s. Thus, Eq. (4) takes the standard form

$$\begin{aligned}
\dot{x}_1 &= x_2 - 1,\\
\dot{x}_2 &= \frac{\varepsilon}{b}\frac{2\sin(s/b)}{x_3}x_2 - \frac{\beta\omega}{b}x_2 - \frac{\omega^2}{b^2}\frac{\sin(x_1+s)}{x_3},\\
\dot{x}_3 &= -\frac{\varepsilon}{b}\sin(s/b),
\end{aligned} \tag{30}$$

where it is assumed that $x_2 - 1$ is of order ε. With the general averaging method we can find the first, second and the following order approximations of Eq. (30).

Resonance rotation domains of the pendulum with periodically varying length for various $|b|$ are presented in Fig. 5. We see that greater values of relative rotational velocities $|b|$ are possible for higher excitation amplitudes ε. Numerically obtained rotational regimes are depicted in Fig. 5 by color points in parameter space (ω, ε) with $\beta = 0.05$ and initial conditions $\theta(0) = \pi, \dot{\theta}(0) = 0.05$. Domains of these points are well bounded below by analytically obtained curves for corresponding $|b|$.

7.1. Rotations with relative velocity $|b| = 1$

It is the third order approximation of averaged equations where regular rotations with $|b| = 1$ can be observed; see Fig. 4(b). In the third order approximation, averaged equations take the following form

$$\begin{aligned}
\dot{\bar{x}}_1 &= \frac{3\varepsilon\omega^2}{4}\left(\cos(\bar{x}_1) - 2\pi\sin(\bar{x}_1)\right) + \left(1 - \frac{3\varepsilon^2}{2}\right)\bar{x}_2 - 1,\\
\dot{\bar{x}}_2 &= -\frac{3\varepsilon\omega^2}{2}(1-2\varepsilon)\sin(\bar{x}_1) - \beta\omega\bar{x}_2
\end{aligned} \tag{31}$$

where $\bar{x}_1$ and $\bar{x}_2$ are the averaged slow variables x_1 and x_2. Auxiliary variable $x_3 = 1 + \varepsilon\cos(s/b)$ has unit average $\bar{x}_3 = 1$ and is excluded from the consideration. Excluding variable $\bar{x}_2$ from the steady state conditions $\dot{\bar{x}}_1 = 0$ and $\dot{\bar{x}}_2 = 0$ in (31) we obtain the equation for the averaged phase mismatch $\bar{x}_1$

$$\begin{aligned}
&3\varepsilon\omega\left(2 - 4\varepsilon + 2\omega\beta\pi - 3\varepsilon^2 + 6\varepsilon^3\right)\sin(\bar{x}_1)\\
&\quad - 3\varepsilon\omega^2\beta\cos(\bar{x}_1) + 4\beta = 0,
\end{aligned} \tag{32}$$

which after dividing by

$$3\varepsilon\omega\sqrt{\left(2 - 4\varepsilon + 2\omega\beta\pi - 3\varepsilon^2 + 6\varepsilon^3\right)^2 + \omega^2\beta^2}$$

can be transformed to the following

$$\sin(\bar{x}_1 + \vartheta) = \frac{-4\beta}{3\varepsilon\omega\sqrt{\left(2 - 4\varepsilon + 2\omega\beta\pi - 3\varepsilon^2 + 6\varepsilon^3\right)^2 + \omega^2\beta^2}}, \tag{33}$$

where $\vartheta = (-1)^j \arcsin\left(\frac{\omega\beta}{\sqrt{\left(2-4\varepsilon+2\omega\beta\pi-3\varepsilon^2+6\varepsilon^3\right)^2+\omega^2\beta^2}}\right) + \pi j$ with j being an integer number. Thus, it is clearly seen from (33) that Eq. (32) has a solution only if

$$9\varepsilon^2\omega^2\left(2 - 4\varepsilon + 2\omega\beta\pi - 3\varepsilon^2 + 6\varepsilon^3\right)^2 + 9\varepsilon^2\omega^4\beta^2 \geq 16\,\beta^2. \tag{34}$$

Inequality (34) gives the equation for the boundary of the domain in parameter space, where rotations with $|b| = 1$ can exist. This boundary is depicted with a bold dashed line in Fig. 5 on the parameter plane (ω, ε) for $\beta = 0.05$ and $\varepsilon < 0.25$. Omitting higher order terms the expression of the boundary can be reduced to $\varepsilon = \frac{2\beta}{3\omega}$.

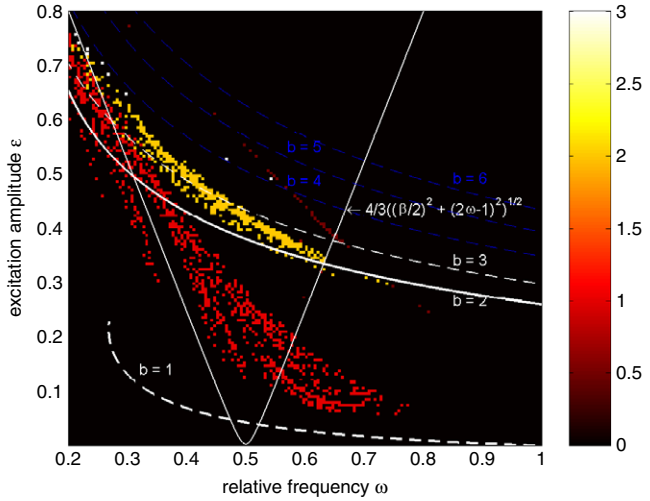

Fig. 5. Absolute values of relative rotational velocities are shown with different colors on the plane of parameters ε and ω at damping $\beta = 0.05$. The correspondence between the colors and values is shown by the color bar on the right. (For interpretation of the references to colour in this figure legend, the reader is referred to the web version of this article.)

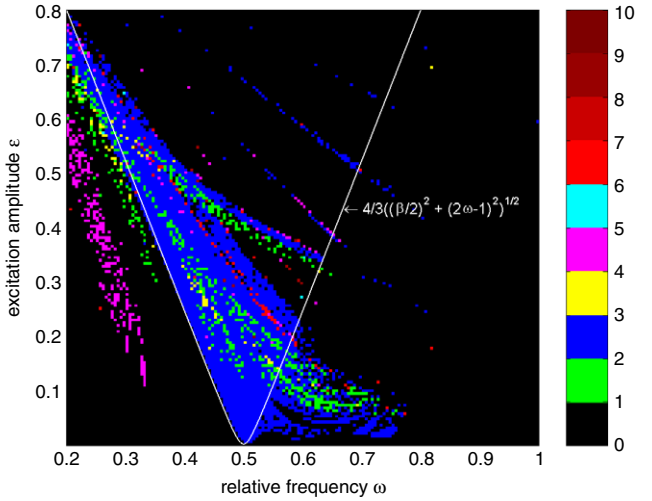

Fig. 6. Periods of regular motions divided by period of excitation are shown with different colors on the parameter plane (ω, ε) at $\beta = 0.05$. The correspondence between the colors and relative periods is shown by the color bar on the right, where stationary and chaotic regimes are shown with black color.

7.2. Rotations with higher relative velocities

Rotations with higher averaged velocities $b = 2, 3, 4, \ldots$ correspond to higher excitation amplitudes ε. That is why we will consider the coefficient $\frac{\omega^2}{b^2}$ being of order $\left(\frac{\varepsilon}{b}\right)^2$, and $\frac{\beta\omega}{b}$ being of order $\left(\frac{\varepsilon}{b}\right)^4$. With this new ordering we obtain the fifth order approximation of the averaged equations for $b = 2$

$$\begin{aligned} \dot{\bar{x}}_1 &= \left(1 - \frac{3}{2}\varepsilon^2 + \frac{67}{12}\varepsilon^4\right)\bar{x}_2 - 1, \\ \dot{\bar{x}}_2 &= \frac{\varepsilon^2\omega^2}{16}\left(6\bar{x}_2 - 1\right)\sin\left(\bar{x}_1\right) - \frac{\beta\omega}{2}\bar{x}_2, \end{aligned} \tag{35}$$

which have steady state solutions determined by the following expressions

$$\begin{aligned} \sin\left(\bar{x}_1\right) &= \frac{8\beta}{5\varepsilon^2\omega}\left[\frac{1}{1 + \frac{3}{10}\varepsilon^2 - \frac{67}{60}\varepsilon^4}\right], \\ \bar{x}_2 &= \frac{1}{\left(1 - \frac{3}{2}\varepsilon^2 + \frac{67}{12}\varepsilon^4\right)}. \end{aligned} \tag{36}$$

Solutions of (36) exist only if $5\varepsilon^2\omega\left(1 + \frac{3}{10}\varepsilon^2 - \frac{67}{60}\varepsilon^4\right) \geq 8\beta$, i.e. the domain of rotations with $|b| = 2$ in the parameter space has the following boundary condition depicted in Fig. 5 with a bold solid line

$$\omega \geq \frac{8\beta}{5\varepsilon^2}\left[\frac{1}{1 + \frac{3}{10}\varepsilon^2 - \frac{67}{60}\varepsilon^4}\right]. \tag{37}$$

Similarly, we can obtain from the fifth order approximation of averaged equations the boundary conditions for higher rotational velocities $|b| = 3, 4, 5, 6$ as

$$\omega \geq \frac{2\beta}{3\varepsilon^2}|b|. \tag{38}$$

These boundaries are shown in Fig. 5 by thin dashed lines.

7.3. Rotations with fractional relative velocities

Similar boundary conditions can also be obtained from approximations of averaged equations of system (30) with fractional relative velocities $|b| = 1/2, 1/4, 3/4, \ldots$. But all such regimes found in numerical simulations include repeating series of clockwise and counterclockwise rotations of the pendulum with periodically varying length. Such a swinging regime can be called the regular rotational–oscillational motion. In that case, variable x_1 is not slow because velocity x_2 has no small amplitude and changes its sign during the period of motion. It does not fit for standard averaging method we used here so far. We believe that the study of rotational–oscillational motion requires more general substantially nonlinear averaging with fast variables which are beyond this study. Note that the regular rotational–oscillational motion can have zero average velocity when numbers of clockwise and counterclockwise rotations are equal. These regimes have also been found numerically; see Fig. 4(d).

7.4. Periods of motion

Averaged equations such as (31) and (35) can satisfy not only steady state solutions but also periodic ones. That is why we observe rotations with periods equal to various integer numbers multiplied by excitation period; see Fig. 6. Regular oscillations occur with periods mostly equal to $2, 4, 8, \ldots$ but there are also relative periods $3, 6, 9$. Here by regular oscillations we refer to the motion during which the pendulum does not pass the upper vertical position.

8. Transition to chaos

We have observed two types of transition to chaos. The first type is when the system goes through the cascade of period doubling (PD) bifurcations occurring within the instability domain of the vertical position when the excitation amplitude ε increases, for example at $\omega = 0.5$ in Figs. 6 and 10. The second type is when chaos immediately appears when the system enters the instability domain of the lower vertical position, for example at $\omega = 0.67$; see Figs. 6 and 7. In order to determine chaos domains we calculated maximal Lyapunov exponents presented in Fig. 8. We recall that positive Lyapunov exponents correspond to chaotic motions. In Fig. 9 the Poincare map is shown, which reveals a typical strange attractor structure. Note that chaotic motion includes passing through the upper vertical position, i.e. irregular oscillations–rotations. This is usually called tumbling chaos.

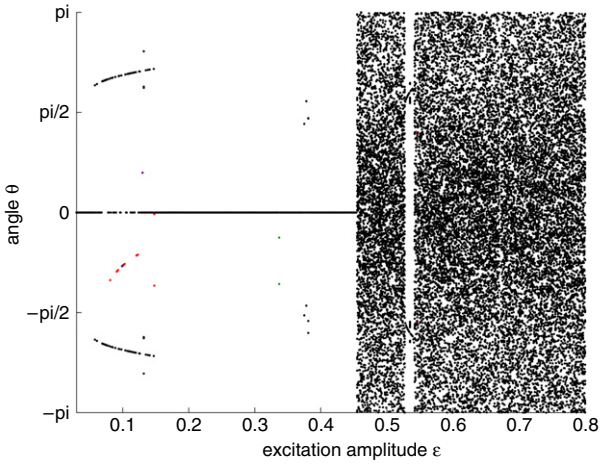

Fig. 7. The bifurcation diagram for the parameters $\omega = 0.67$ and $\beta = 0.05$. After Andronov–Hopf bifurcation (AH) of the vertical equilibrium the chaotic motion occurs immediately.

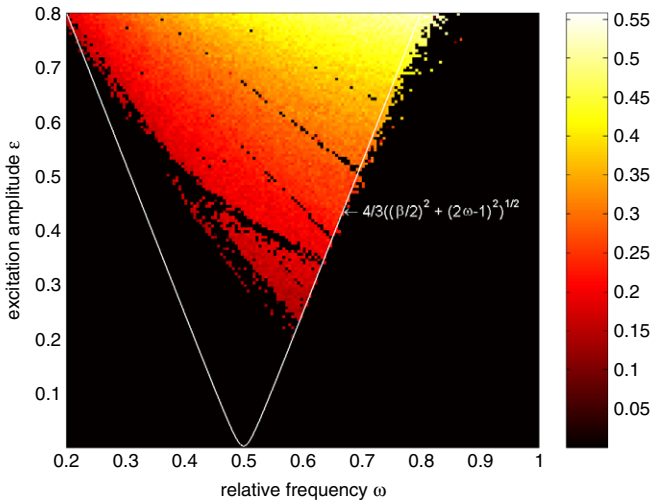

Fig. 8. Maximal Lyapunov exponents are shown with different colors on the plane of parameters ε and ω at the damping $\beta = 0.05$. The correspondence between the colors and values is shown by the color bar on the right, where black color distinguishes the zero maximal Lyapunov exponent which corresponds to a regular regime while lighter colors correspond to positive exponents which characterize chaotic motions. (For interpretation of the references to colour in this figure legend, the reader is referred to the web version of this article.)

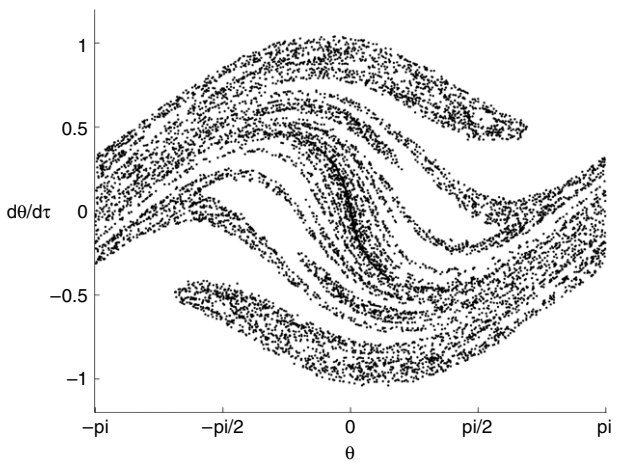

Fig. 9. The Poincare map for the parameters $\varepsilon = 0.255$, $\omega = 0.59$, and $\beta = 0.05$.

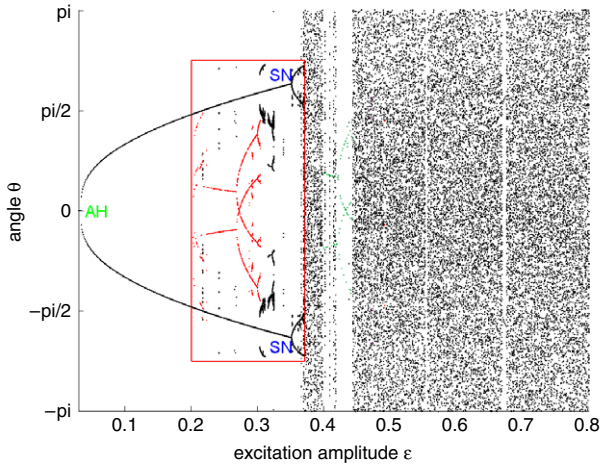

Fig. 10. The bifurcation diagram for the parameters $\omega = 0.5$ and $\beta = 0.05$. After Andronov–Hopf bifurcation (AH) a limit cycle appears which experiences the saddle–node bifurcation (SN). Regular rotations with relative mean angular velocity $|b| = 1$ are denoted by red points and $|b| = 2$ by green. (For interpretation of the references to colour in this figure legend, the reader is referred to the web version of this article.)

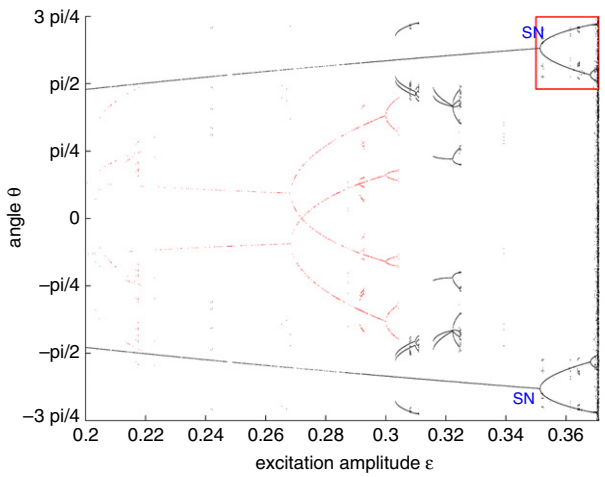

Fig. 11. The bifurcation diagram for the parameters $\omega = 0.5$ and $\beta = 0.05$. Besides a limit cycle with the saddle–node bifurcation (SN) the system has rotational (red points) and rotational–oscillational solutions that lose their stability after the set of the period doubling bifurcations (PD). (For interpretation of the references to colour in this figure legend, the reader is referred to the web version of this article.)

We can see the change of the system dynamics in its route to chaos in the bifurcation diagram shown in Fig. 10, where red points denote rotations with mean angular velocity equal to one excitation frequency and green points denote those equal to two excitation frequencies. The domain with the most complex regular dynamics is surrounded by the rectangle and presented in Fig. 11, where the system can have coexisting oscillations, rotations and rotations–oscillations. In Fig. 12 it is seen that the system goes through the chain of period doubling bifurcations (PD) in its route to chaos.

9. Comparison with the pendulum with oscillating support

There are quite a number of publications on dynamics of the pendulum with oscillating support and fixed length. That is why for the reader who knows some of them, it would be interesting to compare the dynamics of the pendulum with periodically varying length with the pendulum with oscillating support. Both pendula are rich in dynamical regimes, a minute comparison of which

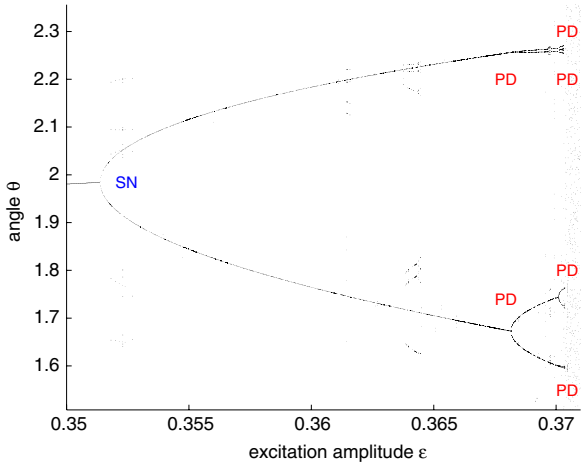

Fig. 12. The bifurcation diagram for the parameters $\omega = 0.5$ and $\beta = 0.05$. After the saddle–node bifurcation (SN) the system goes through the chain of period doubling bifurcations (PD) which precedes the chaotic solution.

deserves a separate study, as we believe. Here we mark out only the striking differences which prove that the pendulum with periodically varying length is a qualitatively separate model.

In the case of zero excitation both pendula can be described by the same equations. But with excitation their equations can coincide only asymptotically in the first approximation if we assume small $\varepsilon \sim \omega^2$ in Eq. (8)

$$\ddot{q} + \beta\omega\dot{q} + \left[\omega^2 - \varepsilon\ddot{\varphi}(\tau)\right] q = 0, \tag{39}$$

where $\ddot{\varphi}(\tau) = -\cos(\tau)$. Small ω implies high excitation frequency Ω. Hence, one would expect the same stabilization phenomenon of inverse vertical position; see e.g. [16]. But, as was mentioned in the introduction, the pendulum with periodically varying length cannot be stabilized in the inverted vertical position. This can be explained by the fact that the vector of the force applied to the mass always passes through the axis of the pendulum. That is why there is no restoring moment to bring the pendulum back to the inverted vertical position after deviation. This observation shows that in general the correct study of stability should be done without any simplification with respect to the parameters of the equation.

It is shown in Section 3 that the second resonance domain is empty, and the numerical results confirm this conclusion; see Fig. 2. It is not the case for the pendulum with oscillating support. More than that, based on numerical analysis the authors suspect that all even resonance domains of the pendulum with periodically varying length are empty.

In Section 7.2 rotations with integer averaged relative velocities b higher than one are found analytically and numerically, and the authors could not find any mention of such fast rotation regimes of the pendulum with oscillating support.

10. Conclusion

Unfairly little studied in the literature the pendulum with periodically varying length exhibits diversity of behavior types. We recognized that the analytical stability boundaries of the vertical position of the swing and the frequency-response curve for limit cycles are in good agreement with the numerical results. The second resonance zone appears to be empty. The stability conditions of limit cycles are derived based on the direct use of Lyapunov's theorem on stability of periodic solutions. We confirm that a pendulum with periodically varying length can be naturally treated as a model of swing. We found numerically regular rotation, oscillation, and rotation–oscillation regimes with various periods and mean angular velocities of the pendulum including high-speed rotations and rotations with fractional relative velocities. We derived analytically the conditions for existence of regular rotation and oscillation regimes, which agree with the numerical results. Domains for chaotic motions are found and analyzed numerically in the parameter space via calculation of Lyapunov exponents and Poincare maps. It is shown that the limit cycles and regular rotations can coexist with the stable stationary attractor in contrast with the chaotic regimes which occur only inside the instability domain of the vertical position. Comparison with the pendulum with oscillating support and fixed length showed the distinctive dynamical features of the pendulum with periodically varying length such as high-speed regular rotations and absence of second instability domain.

Acknowledgement

This research is supported by INTAS grant No. 06-1000013-9019. A part of these results were presented at the 6th EUROMECH Nonlinear Dynamics Conference [17].

Appendix

The standard averaging method is a straightforward procedure and in the literature [2,15] usually only two first approximations are written down. We use the averaging method down to the fifth approximation and feel obliged to present the resulting formulas.

The standard averaging method finds the transformation of the equation system with small and 2π time periodic right hand side

$$\dot{x} = X_1(x,t) + X_2(x,t) + \cdots + X_5(x,t), \tag{40}$$

into an autonomous system (also called the averaged system) which could be solved analytically

$$\dot{\xi} = \xi + \Theta_1(\xi) + \Theta_2(\xi) + \cdots + \Theta_5(\xi) + \cdots, \tag{41}$$

where the lower index denotes the order of smallness with respect to one. A new variable ξ is presented in the following series

$$x = \xi + u_1(\xi,t) + u_2(\xi,t) + \cdots + u_5(\xi,t) + \cdots, \tag{42}$$

which is the approximate solution of system (40) and, hence, of the transformed system (41). The functions u_i and Θ_i can be found one by one after differentiating (42) with respect to time, substituting there expressions (40) and (41), expanding the functions X_i around ξ into Taylor's series, and collecting there terms of the same order.

The averaging operator is defined as follows

$$\langle\cdot\rangle = \lim_{T\to\infty}\frac{1}{T}\int_0^T \cdot|_{x=\xi}\,\mathrm{d}\tau = \frac{1}{2\pi}\int_0^{2\pi} \cdot|_{x=\xi}\,\mathrm{d}\tau.$$

We also define integral operator $\{\cdot\}$ with the following expression

$$\{X(x,\tau)\} = \int \left(X(x,\tau) - \langle X(x,\tau)\rangle\right)\mathrm{d}\tau,$$

which is such an antiderivative that satisfies the condition $\langle\{X(x,\tau)\}\rangle = \{\langle X(x,\tau)\rangle\} = 0$. The latter condition is necessary to obviate an ambiguity. We define following vector product operators

$$Xu_k = \sum_{i=1}^{n}\frac{\partial X}{\partial x_i}u_k^i, \qquad Xu_{k,m} = \sum_{i,j=1}^{n}\frac{\partial^2 X}{\partial x_i\partial x_j}u_k^i u_m^j, \quad \ldots$$

and so on, where i and j are the indices of vector components placed

in u_k^i and u_m^j on the top, not to confuse it with smallness order indices k and m; n is the length of vectors X, u_k and u_m. Hence, we can write recurrent expressions

$$
\begin{aligned}
&\Theta_1 = \langle X_1 \rangle\,, \qquad u_1 = \{X_1\}\,,\\
&\Theta_2 = \langle X_2 + X_1 u_1 \rangle\,, \qquad u_2 = \{X_2 + X_1 u_1 - u_1 \Theta_1\}\,,\\
&\Theta_3 = \left\langle X_3 + X_1 u_2 + X_2 u_1 + \frac{1}{2} X_1 u_{1,1} \right\rangle,\\
&u_3 = \left\{ X_3 + X_1 u_2 + X_2 u_1 + \frac{1}{2} X_1 u_{1,1} - u_1 \Theta_2 - u_2 \Theta_1 \right\},\\
&\Theta_4 = \left\langle X_4 + X_1 u_3 + X_2 u_2 + X_3 u_1 + X_1 u_{1,2} + \frac{1}{2} X_2 u_{1,1} \right.\\
&\qquad \left. + \frac{1}{6} X_1 u_{1,1,1} \right\rangle,\\
&u_4 = \left\{ X_4 + X_1 u_3 + X_2 u_2 + X_3 u_1 + X_1 u_{1,2} + \frac{1}{2} X_2 u_{1,1} \right.\\
&\qquad \left. + \frac{1}{6} X_1 u_{1,1,1} - u_1 \Theta_3 - u_2 \Theta_2 - u_3 \Theta_1 \right\},\\
&\Theta_5 = \left\langle X_5 + X_1 u_4 + X_2 u_3 + X_3 u_2 + X_4 u_1 + X_1 u_{1,3} + X_2 u_{1,2} \right.\\
&\qquad + \frac{1}{2} X_1 u_{2,2} + \frac{1}{2} X_3 u_{1,1} + \frac{1}{2} X_1 u_{1,1,2}\\
&\qquad \left. + \frac{1}{6} X_2 u_{1,1,1} + \frac{1}{24} X_1 u_{1,1,1,1} \right\rangle,
\end{aligned}
\tag{43}
$$

where we similarly denote $u_k \Theta_m = \sum_{i=1}^{n} \frac{\partial u_k}{\partial x_i} \Theta_m^i$. Thus, knowing the functions Θ_i from expressions (43) we can write averaged system (41), which is simpler than the original system (40). If we solve averaged system (41) we are able to write the approximate solution (42) of system (40) substituting slow variables $\xi(t)$ into the functions $u_i(\xi, t)$ obtained from (43). Since the functions $u_i(\xi, t)$ are periodic with respect to time t the behavior of slow variables determines the behavior of the approximate solution. It means that we can study stability of the approximate solutions by stability of the regular solutions of averaged system (41).

References

[1] H. Kauderer, Nichtlineare Mechanik, Springer, Berlin, 1958.
[2] N.N. Bogolyubov, Yu.A. Mitropolsky, Asymptotic Methods in the Theory of Nonlinear Oscillations, Gordon and Breach, New York, 1961.
[3] Ya.G. Panovko, I.I. Gubanova, Stability and Oscillations of Elastic Systems. Modern Concepts, Paradoxes and Mistakes, Nauka, Moscow, 1987.
[4] K. Magnus, Schwingungen. Eine Einfuhrung in die theoretische Behandlung von Schwingungensproblemen, J.Teubner, Stuttgart, 1976.
[5] V.V. Bolotin, Vibrations in Engineering. A Handbook, in: Oscillations of Linear Systems, vol. 1, Mashinostroenie, Moscow, 1999.
[6] A.P. Seyranian, The swing: Parametric resonance, J. Appl. Math. Mech. 68 (5) (2004) 757–764.
[7] M.F. Pinsky, A.A. Zevin, Oscillations of a pendulum with a periodically varying length and a model of swing, Int. J. Non-Linear Mech. 34 (1999) 105–109.
[8] A.A. Zevin, L.A. Filonenko, Qualitative study of oscillations of a pendulum with periodically varying length and a mathematical model of swing, J. Appl. Math. Mech. 71 (6) (2007) 989–1003.
[9] W. Szemplinska-Stupnicka, E. Tyrkiel, A. Zubrzycki, The global bifurcations that lead to transient tumbling chaos in a parametrically driven pendulum, Internat. J. Bifur. Chaos 10 (9) (2000) 2161–2175.
[10] Xu Xu, M. Wiercigroch, M.P. Cartmell, Rotating orbits of a parametrically-excited pendulum, Chaos Solitons Fractals 23 (2005) 1537–1548.
[11] S. Lenci, E. Pavlovskaia, G. Rega, M. Wiercigroch, Rotating solutions and stability of parametric pendulum by perturbation method, J. Sound Vibration 310 (2008) 243–259.
[12] A.P. Seyranian, Resonance domains for the Hill equation with allowance for damping, Doklady Phys. 46 (1) (2001) 41–44.
[13] A.P. Seyranian, A.A. Mailybaev, Multiparameter Stability Theory with Mechanical Applications, World Scientific, New Jersey, 2003.
[14] J.J. Thomsen, Vibrations and Stability. Advanced Theory, Analysis and Tools, Springer, Berlin, 2003.
[15] V.M. Volosov, B.I. Morgunov, Averaging Method in the Theory of Nonlinear Oscillatory Systems, MSU, Moscow, 1971.
[16] A.A Seyranian, A.P. Seyranian, The stability of an inverted pendulum with a vibrating suspension point, J. Appl. Math. Mech. 70 (2006) 754–761.
[17] A.O. Belyakov, A.P. Seyranian, A. Luongo, Regular and chaotic dynamics of the swing, in: Proceedings of the 6th EUROMECH Nonlinear Dynamics Conference, June 30 – July 4, Saint Petersburg, Russia, 2008.